Supporting Information

High-Performance Transparent Copper Grid Electrodes Fabricated by Microcontact Lithography for Organic Photovoltaics

Philip Bellchambers,[a] *Silvia Varagnolo,*[a] *Corinne Maltby,*[b] *Ross A. Hatton**[a]
[a] *Department of Chemistry, University of Warwick, Coventry, CV4 7AL, UK*
[b] *School of Engineering, University of Warwick, Coventry, CV4 7AL, UK*
** Ross.Hatton@warwick.ac.uk*

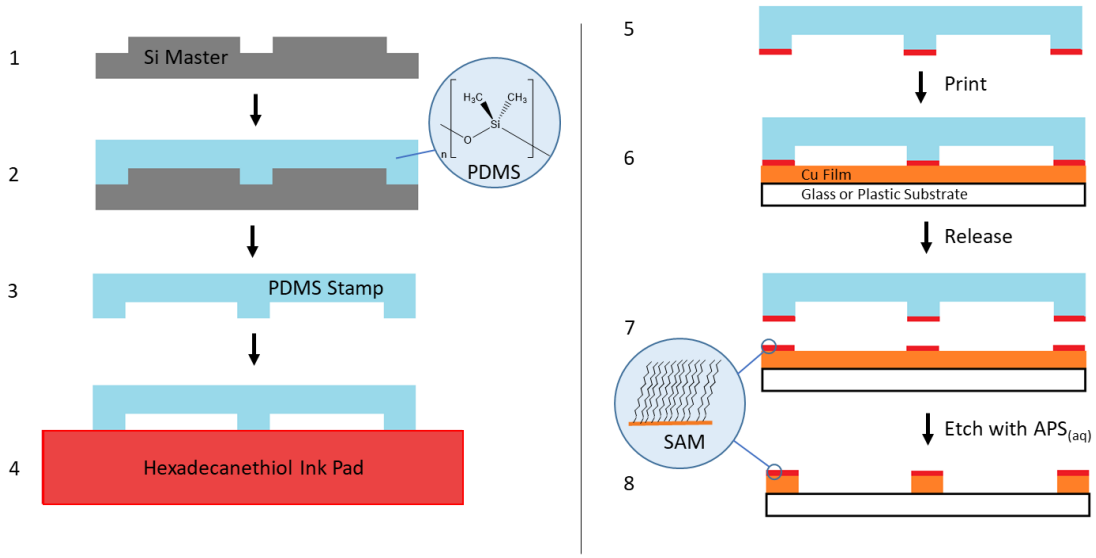

Figure S1: Schematic of the Cu grid fabrication process. Steps 1 - 4 depict the fabrication of the PDMS elastomer stamp from the patterned silicon master, and subsequent inking with HDT from a dilute solution. Steps 5-8 describe the fabrication of a patterned Cu film from the PDMS stamp infused with HDT. The high purity of the HDT ink allows reuse of each PDMS stamp > 100 times without notable deterioration of the replicated pattern in this work.

Equation	y = a + b*x
Plot	Average Transparency / %
Weight	No Weighting
Intercept	75.11414 ± 1.23934
Slope	1.8189 ± 0.20197
Residual Sum of Squares	2.0542
Pearson's r	0.98789
R-Square(COD)	0.97593
Adj. R-Square	0.9639

Table S1. Linear fit parameters for the best-fit line in Figure 1.

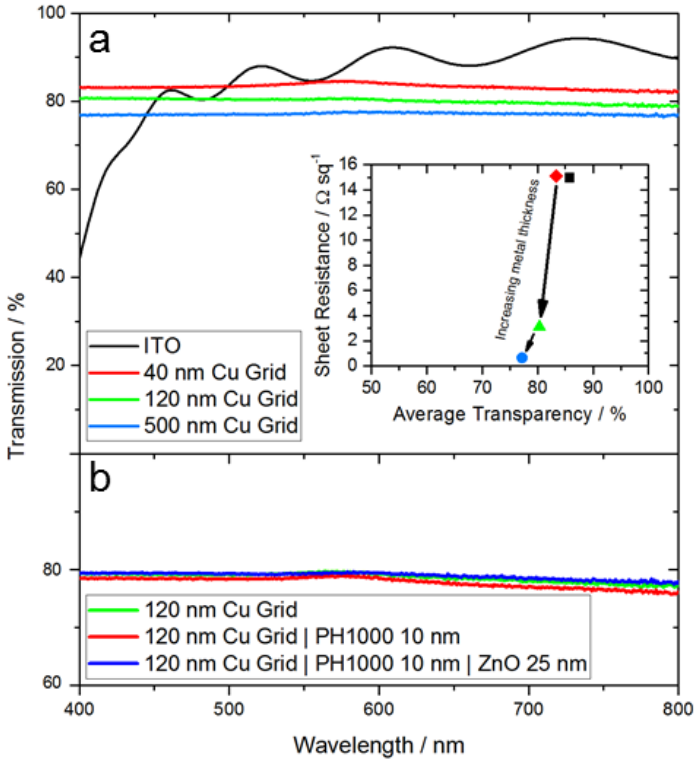

Figure S2. (a) Electronic absorption spectra with the air-substrate interface subtracted for Cu grids with different line thicknesses. The small decrease in transparency when going from a metal thickness of 40 to 120 nm can be understood in terms of the loss in transparency of the Cu gridlines themselves, since at a thickness of 40 nm Cu films are semi-transparent. The reason for the further reduction in transparency when going from 120 nm to 500 nm is not yet clear, although a thickness of 500 nm is not deemed necessary for application in OPVs. Inset shows the relationship between metal thickness and the average transparency/sheet resistance. **b)**

Electronic absorption spectrum of a Cu grid with 120 nm line thickness, with no overlayers (Green), 10 nm PEDOT:PSS (Red) and PEDOT:PSS | 25 nm ZnO (Blue).

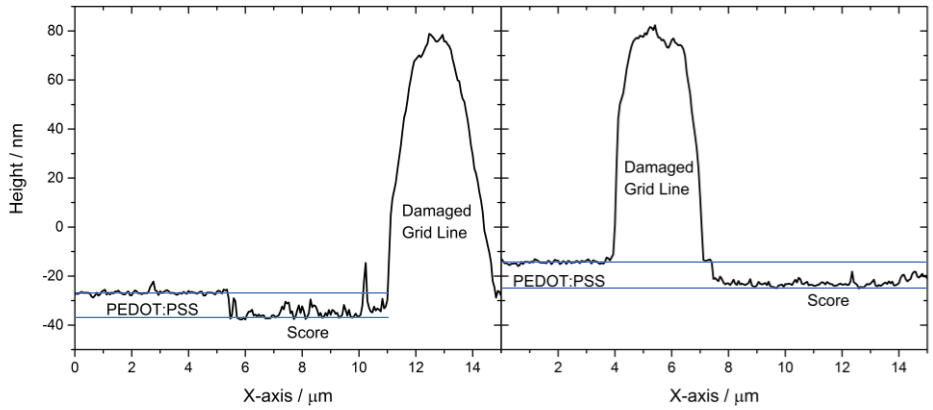

Figure S3. AFM profiles of a scored Cu grid coated with PEDOT:PSS, from which the PEDOT:PSS film thickness is determined to be ~ 10 nm. Blue lines are to guide the eye only. The Cu grid cross-section has rounded, rather than square, edges which is caused by the sharp scoring impliment passing over the grid line.

Electrode	**Haacke figure-of-merit** ($T_{550\ nm}^{10}$ / R_{sh})	**Alternative figure-of-merit** ($T_{average(400\text{-}800\ nm)}^{10}$ / R_{sh})
Cu grid, pitch 27.3 μm	0.031	0.036
Cu grid, pitch 27.3 μm (after annealing)	0.048	0.046
Cu grid, pitch 40 μm	0.041	0.035
Cu grid, pitch 75 μm	0.044	0.042
Cu grid, pitch 150 μm	0.047	0.046
ITO on glass	**0.040**	0.024
ITO on PEN	0.013	0.014

Table S2. Summary of Haacke figure-of-merit (transmittance^{10} / sheet resistance) for the transparent electrodes in this study. All are referenced to the bare substrate to exclude reflection.

Device Area	Electrode	J_{sc} / mA cm^{-2}	V_{oc} / V	FF	PCE / %
Small (0.06 cm^2)	ITO glass (15 Ω sq^{-1})	14.10 ± 0.68 (*14.27*)	0.84 ± 0.00 (*0.86*)	0.64 ± 0.03 (*0.69*)	7.54 ± 0.37 (*8.48*)
Large (0.60 cm^2)	ITO glass (15 Ω sq-1)	14.53 ± 0.24 (14.67)	0.88 ± 0.01 (0.89)	0.55 ± 0.04 (0.60)	7.12 ± 0.64 (7.86)
Small (0.06 cm^2)	40 nm Cu Grid (15.1 Ω sq^{-1}) | PEDOT:PSS	12.32 ± 0.43 (*12.53*)	0.86 ± 0.01 (*0.86*)	0.67 ± 0.04 (*0.70*)	7.03 ± 0.61 (*7.55*)
Large (0.60 cm^2)	40 nm Cu Grid (15.1 Ω sq^{-1}) | PEDOT:PSS	10.90 ± 2.01 *(11.91)*	0.87 ± 0.01 *(0.87)*	0.51 ± 0.06 *(0.59)*	4.82 ± 1.08 *(6.14)*
Small (0.06 cm^2)	120 nm Cu Grid (3.2 Ω sq^{-1}) | PEDOT:PSS	11.31 ± 0.56 *(11.80)*	0.84 ± 0.02 *(0.86)*	0.63 ± 0.07 *(0.70)*	6.03 ± 0.79 *(7.08)*
Large (0.60 cm^2)	120 nm Cu Grid (3.2 Ω sq-1) | PEDOT:PSS	11.63 ± 0.45 *(12.48)*	0.88 ± 0.01 *(0.90)*	0.63 ± 0.03 *(0.66)*	6.49 ± 0.49 *(7.26)*
Small (0.06 cm^2)	Highly Flexible 120 nm Cu Grid (PET substrate) | PEDOT:PSS	11.29 ± 0.30 *(11.67)*	0.85 ± 0.03 *(0.87)*	0.61 ± 0.04 *(0.65)*	5.83 ± 0.55 *(6.61)*
Small (0.06 cm^2)	10 nm PEDOT:PSS	0.07 ± 0.03 *(0.10)*	0.69 ± 0.20 (*0.87*)	0.25 ± 0.00 (*0.25*)	0.01 ± 0.01 (*0.02*)
Small (0.06 cm^2)	Flexible ITO (PEN substrate)	13.63 ± 0.53 (*14.01*)	0.77 ± 0.12 (*0.86*)	0.52 ± 0.09 (*0.65*)	5.61 ± 1.82 (*7.84*)

Table S3. A series of devices with the structure Electrode | Al-doped ZnO (25 nm) | PBDB-T / ITIC | MoO_3 (6 nm) | Al where both electrode design and active area are varied. Mean ± Standard Deviation (Champion).

Electrode	Jsc / mA cm^{-2}	V_{oc} / V	FF	PCE / %
ITO	17.7 ± 0.4 (18.2)	0.82 ± 0.01 (0.82)	0.69 ± 0.03 (0.72)	10.1 ± 0.6 (10.8)
Cu Grid, Pitch: 27.3 μm	12.4 ± 0.4 (12.8)	0.80 ± 0.01 (0.81)	0.69 ± 0.01 (0.71)	6.9 ± 0.3 (7.4)
Cu Grid, Pitch: 50 μm	15.5 ± 0.5 (15.7)	0.80 ± 0.01 (0.81)	0.67 ± 0.02 (0.69)	8.4 ± 0.4 (8.7)
Cu Grid, Pitch: 75 μm	16.2 ± 1.1 (17.4)	0.80 ± 0.01 (0.80)	0.67 ± 0.02 (0.67)	8.6 ± 0.4 (9.3)
Cu Grid, Pitch: 150 μm	17.0 ± 0.3 (17.5)	0.81 ± 0.01 (0.81)	0.65 ± 0.02 (0.67)	9.0 ± 0.4 (9.4)

Table S4. A series of devices with the structure Electrode | Al-doped ZnO (25 nm) | PBDB-T-2Cl/ITIC-2F | MoO_3 (6 nm) | Al where the grid electrode pitch is varied. Mean ± Standard Deviation (Champion).

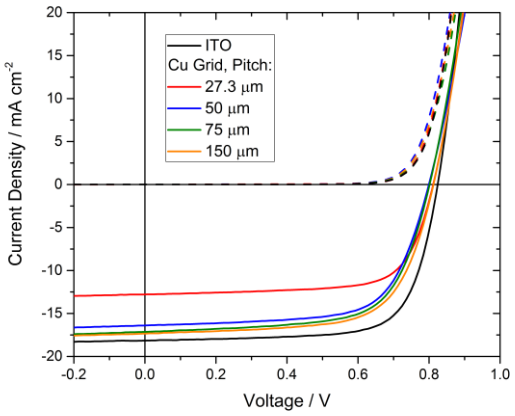

Figure S4. Champion device characteristics for Cu grid devices with varying pitch in the structure: Grid | ZnO | PBDB-T-2Cl/ITIC-2F | MoO_3 | Al.

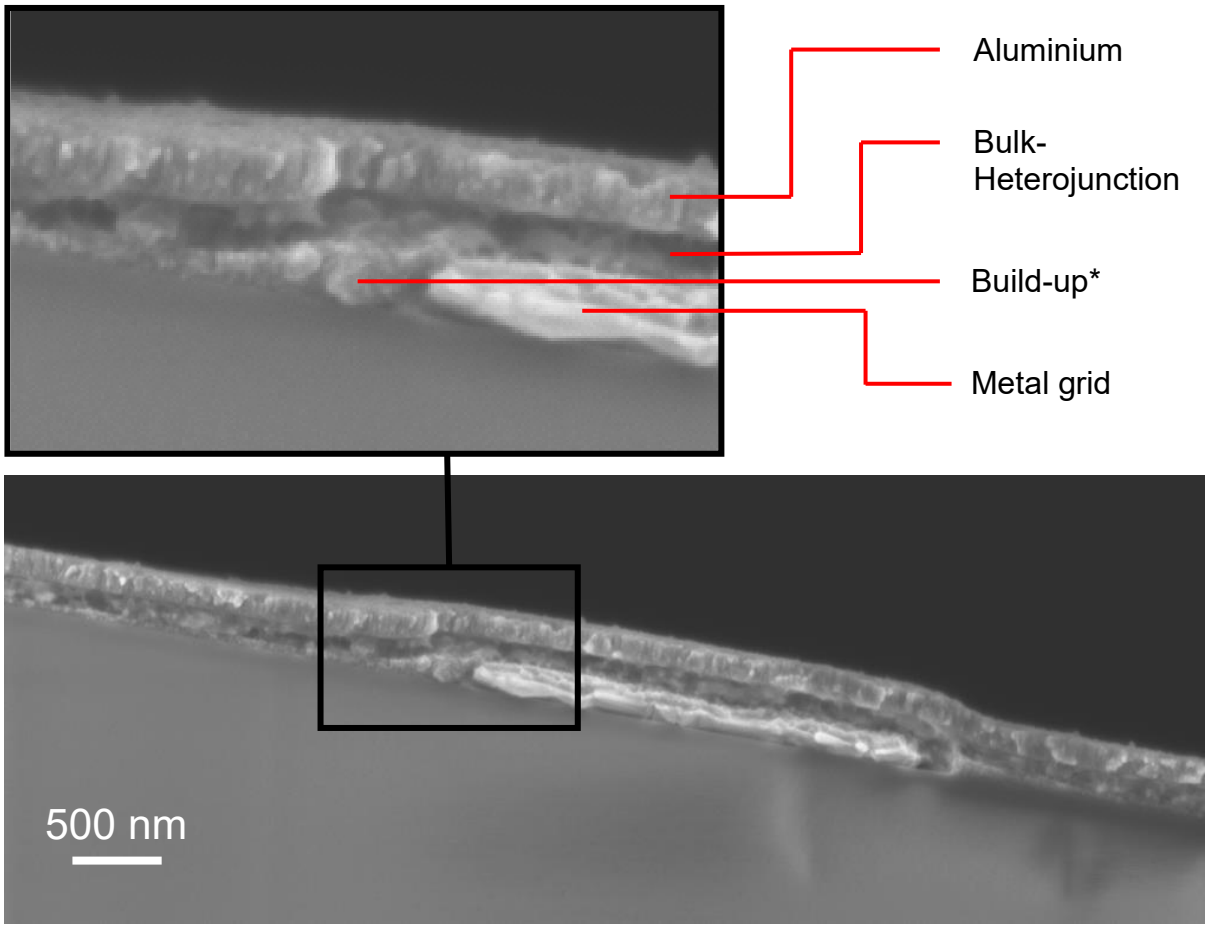

Figure S5. Cross-sectional SEM image of an OPV device with the structure: Cu grid electrode (120 nm grid height) | PEDOT:PSS (10 nm) | Al-doped ZnO (25 nm) | PBDB-T / ITIC | MoO_3 (6 nm) | Al (150 nm) with expanded section (upper) showing the build-up (accumulation) of ZnO | PEDOT:PSS at the sharp edge between the glass substrate and metal grid line, which serves to smooth the sharp interface at the edge of the copper grid lines so that the photoactive organic semiconductor layer is of uniform thickness.

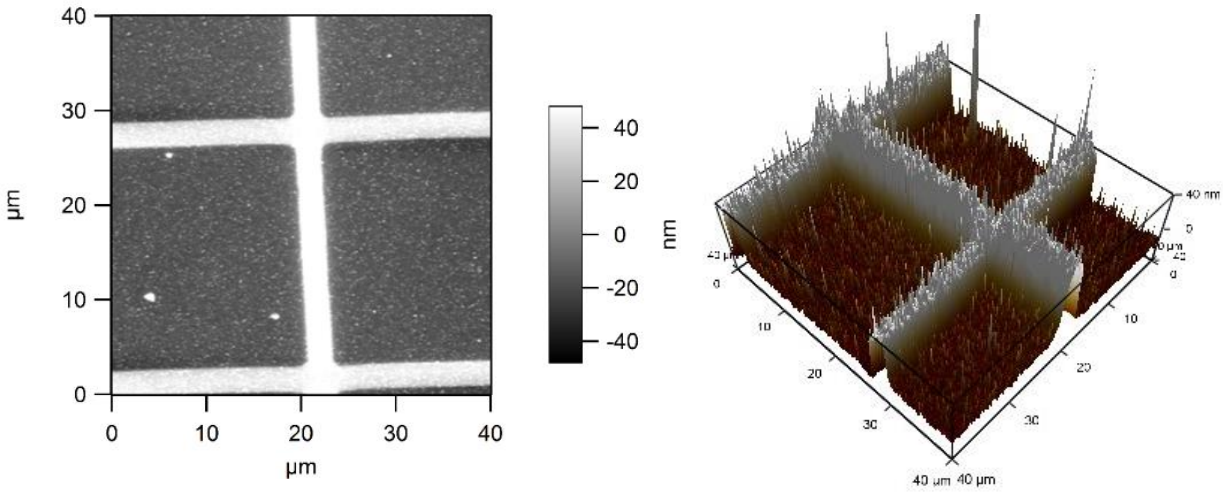

Figure S6. (Left) AFM topographic image of the surface of an OPV device with the structure glass | 110 nm Cu Grid electrode | PEDOT:PSS 10 nm | ZnO 25 nm | Bulk-heterojunction | MoO_3 6 nm | Al 150 nm. (Right) 3D depiction of the same image.

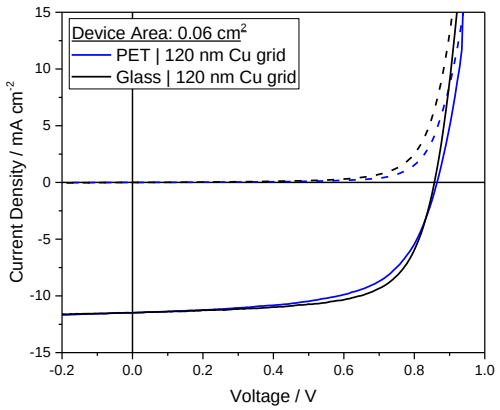

Figure S7. A comparison of the chamion OPV device with structure: 120 nm Cu grid | Al-doped ZnO (25 nm) | PBDB-T / ITIC | MoO_3 (6 nm) | Al, supported on plastic (PET, blue) and glass (black) respectively.

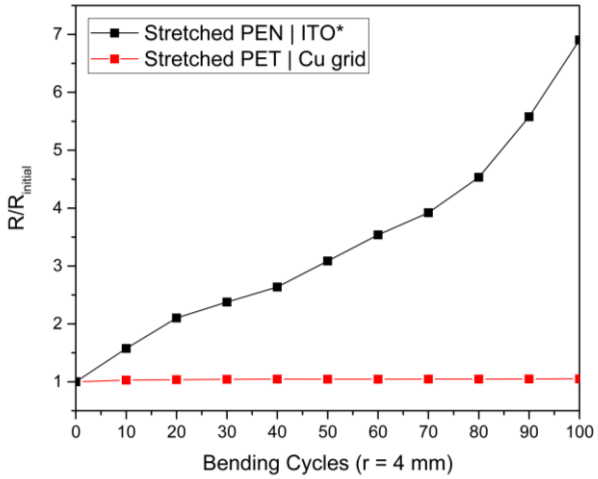

Figure 8. Normalised sheet resistance for commercial ITO on PEN and a 40 nm Cu grid on PET as a function of the number of bends through a tight radius of 4 mm.

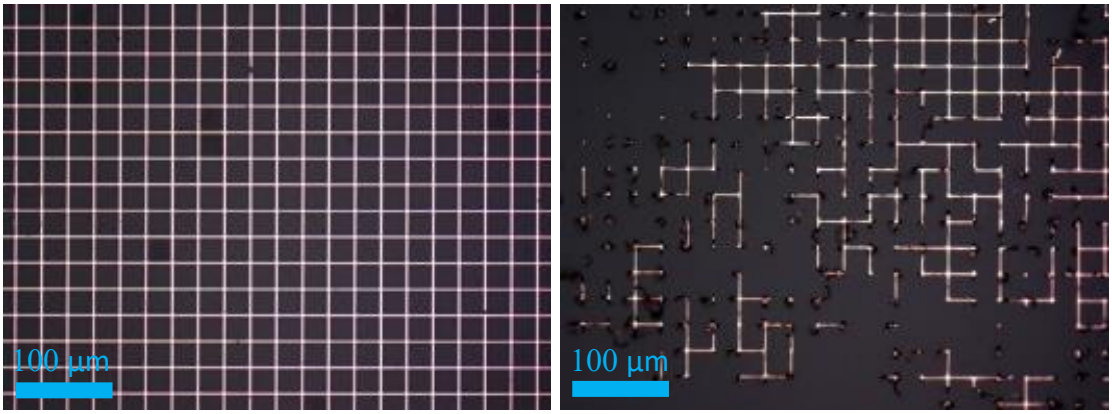

Figure S9. 120 nm Cu grid electrodes after 30 minutes ultra-sonication in DI water on glass derivatised with MPTMS & APTMS vapours (left) and plain glass (right).

Sample#	Height before 30s acetic acid rinse / nm		Sample average Height		Collective average / nm	Standard Deviation
S1	128	127.3	127.7		127.4	1.2
S2	128.2	127.4	127.8			
S3	128.4	125.2	126.8			
Sample#	**Height after 30s acetic acid rinse / nm**		**Sample average Height**		**Collective average / nm**	**Standard Deviation**
S1	124.2	124.6	124.4		122.8	1.8
S2	123.1	119.6	121.35			
S3	122	123.1	122.55			

Table S5. The measured heights of a set of 120 thick Cu grids which have been exposed to ambient air for 160 days before and after a 30s acetic acid rinse, which selectively removes the oxide overlayer calculated at 4.7 nm thick. The sheet resistance of each sample did not change during the process, affirming the selectivity of the acetic acid for copper oxides.